The Quest for Inorganic Fullerenes

Susanne Pietsch[1], Andreas Dollinger[1], Christoph H. Strobel[1], Eun Ji Park[1,] Gerd Ganteför[1*]

Hyun Ook Seo[3], Young Dok Kim[2*]

Juan - Carlos Idrobo[4], Stephen J. Pennycook[5]

[1]Department of Physics, University of Konstanz, D-78457 Konstanz, Germany

[2] Department of Chemistry, Sungkyunkwan University, 440-746 Suwon, Republic of Korea

[3]Center for Free-Electron Laser Science/DESY, D-22607 Hamburg, Germany

[4] Center for Nanophase Materials Sciences, Oak Ridge National Laboratory, Oak Ridge, Tennessee 37831, USA.

[5] Department of Materials Science and Engineering, National University of Singapore, Singapore 117575

Abstract

Experimental results of the search for inorganic fullerenes are presented. $Mo_nS_m^-$ and $W_nS_m^-$ clusters are generated with a pulsed arc cluster ion source equipped with an annealing stage. This is known to enhance fullerene formation in the case of carbon. Analogous to carbon, the mass spectra of the metal chalcogenide clusters produced in this way exhibit a bimodal structure. The species in the first maximum at low mass are known to be platelets. Here, the structure of the species in the second maximum is studied by anion photoelectron spectroscopy, scanning transmission electron microscopy and scanning tunneling microcopy. All experimental results indicate a 2-dimensional structure of these species and disagree with a 3-dimensional fullerene-like geometry. A possible explanation for this preference of 2-dimensional structures is the ability of a two-element material to saturate the dangling bonds at the edges of a platelet by excess atoms of one element. A platelet consisting of a single element only cannot do this. Accordingly, graphite might be the only material forming nano-spheres because it is the only single element layered material.

Key Words: Mass-selected clusters; Inorganic Fullerenes, MoS_2, WS_2,

1. Introduction

Nanoparticles and clusters have unique physical and chemical properties that make them interesting for basic research as well as applications. Perhaps the best known clusters are the carbon fullerenes [1]. These are hollow spheres of pure carbon, which are available in various sizes. The driving force for the formation of such spheres is the energetic unfavorable position of carbon atoms at the edges of graphene planes. For a graphene flake it is therefore advantageous to curve itself into a sphere, so that there is no edge. The most stable fullerenes are C_{60} and C_{70}, but there is a variety of other sizes, from which a manifold of carbon-derived materials can by synthesized. Additional atoms or clusters can be stored in the hollow spheres (endohedral) stabilizing the fullerenes even further [2]. The question might be raised whether there are other materials forming hollow nano-spheres. In principle, all 2-dimensional materials [3] consisting of weakly interacting monomolecular planes could behave similarly. However, until today no so-called inorganic fullerenes have been found. There are many materials that form nanotubes and nested fullerenes similar to carbon [4-15], but so far no "single-wall" nano-spheres analogous to C_{60} and C_{70} have been observed.

MoS_2 and WS_2 are layered materials which exhibit a certain similarity to carbon [3]. Both are used as lubricants, because the weak van-der-Waals interaction between the layers make these materials soft and friction reducing. Both materials easily form nanotubes again similar to carbon [16]. Also, both materials form nested fullerenes [8, 17], which can be viewed as "multiwall" fullerenes. The smallest such structure seems to have three walls [8, 18]. In contrast to carbon, these structures are not spherical. The smallest ones have octahedral geometries [15]. An octahedron is built from eight planar triangles. Triangular 2-dimensional

nano-platelets of MoS_2 and WS_2 are exceptional stable [19, 20]. There are magic numbers, i.e., triangles with a certain size that are more stable than others. In the gas phase, the most stable platelet is $W_{15}S_{42}$ and the smallest observed platelet is $W_{10}S_{30}$ [21-23]. The octahedral shape of the nested inorganic fullerenes indicates that 2-dimensional triangular structures are preferred by MoS_2 and WS_2. No "single-wall" real fullerenes have been found until today.

Carbon fullerenes have first been discovered in a mass spectrum of clusters generated by a cluster ion source [24, 25]. The material (carbon) is vaporized in a laser pulse and cooled in an inert carrier gas. Condensation results in the formation of dimers and trimers and later larger clusters. A few percent of the clusters are charged allowing the recording of mass spectra. The fullerene mass spectrum exhibits a characteristic bimodal structure. The first maximum at low mass corresponds to the carbon chains and rings, while the second maximum is formed by the fullerenes. Within this second maximum, the mass with 720amu (= C_{60}) stands out. So far, cluster methods have not been used for a systematic search for inorganic fullerenes. Inorganic fullerenes have been synthesized by other techniques suitable for the synthesis of large amounts of material. One common method is the reduction of a metal oxide (MoO_3 or WO_3) in an H_2/H_2S atmosphere [26]. The synthesized particles consist of thousands of atoms and are much larger than carbon fullerenes. With these methods it is difficult to control the condensation process and optimize for the generation of clusters less than 100 atoms. A few attempts have been made to synthesize smaller particles and record mass spectra [27]. However, the results of these earlier experiments do not agree with the data presented here.

We present the results of a search for inorganic fullerenes by using well established methods

of cluster science. Nanoclusters of Mo_nS_m and W_nS_m are synthesized in a cluster ion source at conditions under which in the case of graphite fullerenes are formed [28, 29]. The mass spectra show a bimodal distribution similar to the mass spectra of the carbon fullerenes. It is already known that the particles in the first maximum are one-dimensional chains and two-dimensional platelets [21-23]. Here we focus on the structure determination of the larger clusters in the second maximum. These clusters are studied with anion photoelectron spectroscopy, scanning transmission electron microscopy and scanning tunneling microscopy. All experimental data support the theoretical prediction that these particles do not have a fullerene-like 3d-structure but are 2-dimensional platelets. At the end of the paper it will be discussed, why carbon fullerenes may be the only fullerenes existing.

2. Experimental

Neutral and negatively charged Mo_nS_m and W_nS_m Clusters are generated with a pulsed arc cluster ions source (PACIS) [21-23]. In the past, the source has been used successfully to synthesize all kinds of carbon fullerenes [28, 29]. In contrast to the generation of metal clusters, for the effective generation of carbon fullerenes an annealing stage is necessary [28, 30]. It is mounted on the end of the extender of the source (Fig. 1). The annealing stage is a weak electrical discharge which reheats the carrier gas containing the carbon clusters . In the primary strong electrical discharge huge amounts of carbon are vaporized which condense downstream from the extender. This results in the formation of large graphitic carbon clusters. The annealing heats this ensemble of large clusters up again. Above the mass of C_{30}, which is the minimum size of stable fullerenes under these conditions, fullerenes are practically the only species generated. Without the annealing only very few fullerenes are formed. This technique is now applied to generate inorganic fullerenes.

Metalsulfide clusters are generated by the vaporization of the corresponding metal (W or Mo), while a carefully controlled amount of H_2S is introduced into the PACIS. This method

has been already used successfully to synthesize Mo_nS_m and W_nS_m plateletes and nanowires [21-23]. No indication for hydrogen contamination has been found in the mass spectra or in the photoelectrons spectra. H_2S based methods have been used by other groups searching for inorganic fullerenes and no indications for remaining hydrogen have been found [10, 26]. The metal-sulfur interaction is so dominant that hydrogen is driven off.

The cluster anions are mass-selected by a reflectron time-of-flight mass spectrometer. A selected bunch of anions can be studied by photoelectron spectroscopy. The anions are irradiated by a laser pulse from a F_2-Excimer laser with a photon energy of 7.9eV. This relatively high photon energy is required because of the high electron affinities of the sulfides. The kinetic energy of the detached electrons is measured using a magnetic bottle time-of-flight electron spectrometer. This part of the apparatus is described elsewhere [31].

For studies with a scanning transmission electron microscope, neutral clusters are deposited on a standard TEM grid consisting of a copper grid holding with a thin silicon dioxide membrane (Fig. 1). After deposition the wafer is removed from the vacuum and sent to the STEM group at Oak Ridge National Laboratory [32, 33]. There, the sample is studied with a high resolution aberration corrected scanning transmission electron microscope (STEM). With this instrument it is even possible to identify single atoms. In a different setup, mass-selected clusters are deposited on highly oriented pyrolytic graphite (HOPG). The samples are mounted at the end the reflectron time-of-flight mass-spectrometer. A pulsed mass gate allows controlling the size of the clusters that reach the surface. The kinetic energy of the cluster ions impacting or landing on the surface can be changed by adjusting the sample potential. This is not a sophisticated soft-landing cluster deposition setup, because in the time-of-flight mass spectrometer ions have a rather broad kinetic energy distribution. Hence,

even if a low kinetic energy is selected in an attempt to "soft-land" the clusters, some species still have relatively high kinetic energies and others turn around in the deceleration field before reaching the surface. At such conditions some clusters are soft landed while others impact with considerably excess energy onto the surface. After deposition, the samples are removed from the vacuum and transferred to an ultrahigh vacuum scanning tunneling microscope (STM).

3. Results and Discussion

Fig. 2 displays mass spectra of annealed Mo_nS_m and W_nS_m cluster anions. Without the annealing only one maximum is observed, which starts at low masses and extends up at very high masses (not shown). With the annealing, two maxima are observed. The clusters in the first maximum at low mass have previously been studied by photoelectron spectroscopy [21-23]. The experimental data have been compared to corresponding calculations. These species are 2-dimensional platelets. The position of the second mass spectrum depends on the source conditions (Fig. 3). Several parameters control the average size: the intensity of the main discharge determining the amount of vaporized metal, the amount of H_2S introduced into the source, the amount of Helium and the relative timing of the main discharge and the annealing discharge. In general, with increasing intensity of the main discharge and with increasing amount of H_2S the clusters grow larger. On the other hand, there seems to be a minimum size analogous to the case of carbon fullerenes [28]. If the parameters are optimized to shift the second maximum to mass lower than approx. 80 monomers, this maximum disappears. The minimum size is about 60 MoS_2 or WS_2 monomers. However, there is no clear cut off. The maximum just loses intensity and finally disappears.

The apparent existence of a lower mass limit for the second maximum fits to the hypothesis

that these species might have a 3-dimensional fullerene-like structure. For carbon the lower mass limit of the fullerenes generated with this method is C_{30}. There are smaller fullerenes, but their abundance is extremely low. In principle, the inorganic fullerenes could be either spherical or octahedral. In the spherical particles the monomolecular plane needs to be bent. The smaller the diameter the more energy is required. Alternatively, the particles could be octahedral as indicated by the TEM pictures of nested inorganic fullerenes [8]. Such a cluster can be viewed as eight triangular platelets assembled to an octahedron. For the platelets there is a minimum size. The smallest observed platelet consists of ten MoS_2 units plus a less well defined number of excess sulfur atoms stabilizing the edges (e.g., $Mo_{10}S_{30}$) [22]. This would give a lower limit of 80 MoS_2 units for a hypothetical octahedral cluster. The experiments indicate a lower mass limit of 60 units. Since the lower mass limit for the platelets is very pronounced - there are no smaller platelets in the gas phase - our observation of masses lower than 80 MoS_2 units contradicts the hypothesis of an octahedral 3-dimensional geometry.

The mass resolution is not sufficient to resolve individual cluster sizes within the second maximum. Therefore, a series of photoelectron spectra has been recorded by scanning the mass in equidistant steps over the range covered by the second maximum. The results are displayed in Fig. 4. All photoelectron spectra look similar and are basically featureless. There is a single broad maximum shifting slowly towards higher binding energy with increasing mass. Despite all efforts no hint of a "special" photoelectron spectrum could be found. With the same method C_{60} would have been easily identified because of its large HOMO-LUMO gap. In the anion photoelectron spectra such a gap gives rise to a separate peak at low binding energy. Such a peak would be easily identified in the series of measurements displayed in Fig. 4. However, no such peak has been found. It is possible that such features are too weak, especially if the corresponding cluster anion has a low relative abundance. However, a stable cluster should be one with an enhanced abundance. Therefore, we conclude that our photoelectron data do not support the assumption of the existence of any stable "magic"

species within the second maximum of the mass spectrum.

Since the gas phase studies did not provide any clue on the geometric structure of the species in the second maximum, the clusters are deposited on surfaces and studied with microscopy techniques. In a first attempt the neutral clusters exiting the PACIS in forward direction are deposited on a standard TEM grid. It consists of a Cu grid holding a thin membrane of silicon dioxide (Fig. 1). The source is optimized for maximum production of clusters in the second maximum. Then, the sample is exposed to the neutral beam for 10-60 seconds. Fig. 5 displays three STEM pictures obtained with this method. The deposited material has agglomerated into larger lumps of material. In the two pictures recorded at lower resolution (10nm and 5nm scale bars) material with a layered structure is observed. Such structures are typical for bulk-like WS_2. At highest resolution (2nm scale bar), very small stacks of platelets can be discerned (marked with a circle in the top right corner). All STEM pictures show only 2-dimensional bulk-like structures or structureless amorphous material. Nothing resembling a 3-dimensional fullerene-like structure could be found.

In a final attempt to gain more information about the geometric structure of the species in the second maximum, mass-selected cluster ions have been deposited after passage through the time-of-flight mass spectrometer. There are several difficulties involved into this approach. In the time-of-flight instrument, the anions are accelerated up to 2.5 keV. For deposition the anions need to be decelerated. However, in a time-of-flight instrument the anions do not have a well-defined kinetic energy. Instead, they have a rather broad distribution of kinetic energies. If the anions are decelerated in an electric field before they reach the sample, some species might still have a considerable excess energy of several 100 eV when they hit the surface. Others with low kinetic energy may turn around before reaching the surface. Another difficulty is the extremely low intensity of the deposited

material. Even after running the machine for several hours, only a few clusters could be found on the surface. A pulsed mass gate allows for a mass selection. For intensity reasons, the mass range was selected to cover the full range of the second maximum in the mass spectrum (Fig.2). After deposition, the samples were removed from the vacuum chamber and transferred in air to a scanning tunneling microscope operated in ultrahigh vacuum.

Fig. 6 displays a STM image of cluster anions deposited without deceleration. The kinetic energies are between 3-7eV/atom. The clusters are pinned to surface defects created by the impact. The STM is not able to resolve fine structures within such small particles. However, it is possible to determine the height of particles on flat surfaces with considerable accuracy. The height scans for three particles visible in Fig. 6 are displayed, too. The heights correspond more or less to the height of a single layer of MoS_2 (~ 0,5nm).

The cluster anions can be decelerated prior to deposition. This is achieved by an electric field between the substrate and the last element of the ion optics. If the voltage is set to 2.5keV, practically no anions reach the surface. This is the consequence of the rather broad kinetic energy distribution covering the range between 1.5 and 2.5 keV. Therefore, a lower voltage is selected (2000V) and now clusters with very low energies but also with kinetic energies up to 500eV are deposited. We estimate the kinetic energies to vary between 0 - 3eV/atom. In general, soft landing conditions require a kinetic energy lower than 1eV/atom. But despite our rather undefined deposition conditions now practically no pinned clusters are found on the terraces. Instead, most particles agglomerated at the step edges indicating soft-landing conditions. Fig. 7 displays a high resolution STM image of Mo_nS_m particles bound to a HOPG step edge. It is not possible to extract information about the internal structure of the particles from this picture, but it is possible to measure the height. The height scan provides a value of 0.38 nm. The distance between the outer metal atoms in a single Mo-S-Mo layer is

0.32 nm. Hence, the measured height of the deposited clusters is close to the thickness of a platelet. No cluster with a height significantly exceeding this value has been found in our deposition experiments.

None of our experimental results support the hypothesis of the existence of 3-dimensional fullerene-like Mo_nS_m and W_nS_m clusters in the second maximum of the mass spectrum of the annealed cluster anions. In contrast, the measurements are in full agreement with a 2-dimensional platelet structure. It is still possible that some species in the gas phase do have a 3-dimensional spherical or octahedral structure. But if this is the case, they are so fragile that they are destroyed by the deposition process. However, if the 3-dimensional structure is so fragile, how can it be formed in the rather violent annealing discharge? It seems more likely, that the clusters in the second maximum are just bulk-like clusters consisting of either larger platelets or stacks of smaller platelets as indicated by some of the TEM results (Fig. 5, white circle).

One question remains: Which process is responsible for the appearance of the second maximum? Without the annealing the mass spectrum might extend to very large clusters, which are difficult to be detected by the time-of-flight mass spectrometer. Most likely, the annealing discharge causes strong fragmentation and the large clusters shrink. Therefore, fragmentation of large clusters might give rise to the appearance of the second maximum. This would explain why it is possible to shift the second maximum back and forth by small changes of the source conditions (Fig. 3). If this explanation is correct, the bimodal structure would not be related to a change in the geometric structure. Instead, it would be the result of dynamical growth and fragmentation processes in the source.

We conclude that the clusters in the second maximum of the annealed time-of-flight mass

spectrum most likely are 2-dimensional platelets or stacks of platelets. Apparently there are no fullerene-like single-wall metal chalcogenide clusters. The driving force for a graphene flake to bend itself into a nanosphere are the dangling bonds at the edges of the flake. In the case of the sulfides, surplus sulfur atoms may saturate these dangling bonds. As long as there is the tiniest amount of excess sulfur, stabilization of a 2-dimensional platelet structure might be energetically favorable to the curvature of the platelet. In our experiment it is not possible to control the amount of sulfur so carefully that there is no excess sulfur. A reduction of the sulfur concentration below the stoichiometric required amount results in the formation of metal rich clusters, which have a 3-dimensional compact structure [21]. The system always has the opportunity to respond to a lack of sulfur by the formation of such metal-rich species. Therefore, it might be impossible to force the growth of fullerene-like particles, because there will be always sulfur to stabilize the edges. The other possible hollow structure is an octahedron build from eight triangular platelets. Since the platelets are stable on their own, the bonds between the platelets may be weak. Therefore, single-wall octahedrons might be quite fragile and stacks of platelets may be more stable. Our findings are in agreement with an earlier experimental and theoretical study on small fullerene-like MoS_2 clusters. The calculations predicted that single-wall species might be unstable [15].

2. Conclusion

The driving force for the formation of carbon fullerenes are the dangling bonds at the edges of graphene flakes. To minimize the edge the flake bends itself into a sphere. A similar mechanism might exist for all layered materials such as MoS_2 and WS_2. In an effort to synthesize so-called "inorganic fullerenes", we generated small and medium-size Mo_nS_m and W_nS_m clusters with a cluster source optimized for the production of small carbon fullerenes. Similar to carbon, the very small clusters Mo_nS_m and W_nS_m clusters consisting of less than 30 metal atoms are 2-dimensional. Carbon clusters in this size regime are rings, while the metal chalcogenide clusters are platelets. The structure determination of the larger Mo_nS_m and

W_nS_m clusters with more than 60 metal atoms turned out to be difficult. These clusters have been studied with mass spectroscopy, photoelectron spectroscopy, scanning transmission electron microscopy and scanning tunneling microscopy. Disappointingly, all data indicate a 2-dimensional bulk-like structure of these species similar to the structure of the very small clusters. There are no magic numbers and the mass and photoelectron spectra are featureless. This difference to carbon might be explained by the additional degree of freedom a two-element system has. The edges of MoS_2 and WS_2 flakes can be stabilized by additional sulfur atoms. It is almost impossible to avoid this stabilization in a 2-element condensation process. Hence, it could be that carbon is the only material able to form real fullerenes.

Acknowledgements

Support by German science foundation (Grant No. GA 389/15-1) is gratefully acknowledged. SJP acknowledges support from the US Department of Energy, Materials Science and Engineering Division, and JCI acknowledges support from ORNL's Center for Nanophase Materials Sciences, which is a U.S. Department of Energy, Office of Science User Facility.

References

[1] M. S. Dresselhaus, G. Dresselhaus, and P. C. Eklund, "The Science of Fullerenes and Carbon Nantubes", Academic Press Inc. 1996.

[2] Alexey A. Popov, Shangfeng Yang, and Lothar Dunsch, *Chem. Rev.*, **2013**, *113* (8), pp 5989–6113.

[3] P. Miró, M. Audiffred and T. Heine, Chem. Soc. Rev. 2014, **43**, 6537-6554.

[4] N. G. Chopra, R. J. Luyken, K. Cherrey, V. H. Crespi, M. L. Cohen, S. G. Louie, and A. Zettl, Science **269**, 966 (1995).

[5] Maja Remskar, Ales Mrzel, Z. Skraba, A. Jesih, M. Ceh, J. Demsar, P. Stadelmann, F. Levy, D. Mihailovic, Science **292**, 479 (2001).

[6] R. Tenne, Colloids and Surfaces **A 208** (1–3): 83 (2002).

[7] Y. Q. Zhu, H. W. Kroto, J. Am. Chem. Soc. **125** (5): 1329–1333 (2003).

[8] M.-B. Sadan, L. Houben, A. N. Enyashin, G. Seifert, and R. Tenne, Proc. Natl. Acad. Sci. **105**, 15643 (2008).

[9] R. Tenne, M. Resmkar, A. Enyashin, G. Seifert, Topics in Applied Physics, Volume **111**, 2008, pp 631-671.

[10] R. Tenne and G. Seifert, Annu. Rev. Mat. Res. 2009, **39**, 2.1 - 2.27.

[11] A. Yella, M. Panthöfer, M. Kappl, and W. Tremel, Angew. Chem. Int. Ed. **49** (14), 2575 (2010).

[12] G. Radovsky, R. Popovitz-Biro, M. Staiger, K. Gartsman, C. Thomsen, T. Lorenz, G. Seifert, and R. Tenne, Angew. Chem. Int. Ed. **50** (51), 12316 (2011).

[13] L. Yadgarov, R. Rosentsveig, G. Leitus, A. Albu-Yaron, A. Moshkovich, V. Perfilyev, R. Vasic, A. I. Frenkel, A. N. Enyashin, G. Seifert, L. Rapoport and R. Tenne, Angew. Chem. Int. Ed. **51**, 1148 (2012).

[14] R. Tenne, Frontiers of Physics **9** (3), 370 (2014).

[15] M. Bar-Sadan, A. N. Enyashin, S. Gemming, R. Popovitz-Biro, S. Y. Hong, Yehiam Prior, R. Tenne, and G. Seifert, J. Phys. Chem. B **110**, 25399 (2006).

[16] M. Nath, A. Govindaraj, C. N. R. Rao, Adv. Mat. **13** (4), 283 (2001).

[17] I. Wiesel, H. Arbel, R. Popovitz-Biro, J. M. Gordon, D. Feuermann, R. Tenne, Nano Research, **2** (5) 416 (2009).

[18] P. A. Parilla, A. C. Dillon, K. M. Jones, G. Riker, D. L. Schulz, D. S. Ginley and M. J. Heben, Nature **397**, 114 (1999).

[19] M. V. Bollinger, J. V. Lauritsen, K. W. Jacobsen, J. K. Norskov, S. Helveg and F. Besenbacher, Phys. Rev. Lett. **87**(19), 196803 (2001).

[20] J. V. Lauritsen, J. Kibsgaard, S. Helveg, H. Topsoe, B. S. Clausen, E. Laegsgaard and F. Besenbacher, Nat. Nanotechnol. **2**(1), 53 (2007).

[21] N. Bertram, Y. D. Kim, G. Ganteför, Q. Sun, P. Jena, J. Tamuliene and G. Seifert, Chem. Phys. Lett. **396**, 341(2004).

[22] N. Bertram, J. Cordes, Young Dok Kim, S. Gemming, G. Seifert, G. Ganteför, Chem. Phys. Lett. **418**, 36 (2006).

[23] S. Gemming, J. Tamuliene, G. Seifert, N. Bertram, Y.D. Kim, and G. Ganteför, App. Phys. A **82**, 161 (2006).

[24] E. A. Rohlfing, D. M. Cox, and A. Kaldor, J. Chem. Phys. **81,** 3322 (1984).

[25] H. Kroto, J. R. Heath, S. C. O'Brien, R. F. Curl, and R. E. Smalley, *Nature* **318,** 162 (1985).

[26] Y. Feldman, E. Wassermann, D. J. Srolovitz, R. Tenne, Science **267**, 222 (1995).

[27] D. M. David Jeba Singh, T. Pradeep, Joydeep Bhattacharjee, and U. V. Waghmare, J. Phys. Chem. A **109**, 7339 (2005).

[28] H. Handschuh, G. Ganteför, B. Kessler, P. S. Bechthold, and W. Eberhardt, Phys. Rev. Lett. **74**, 1095 (1995).

[29] O. Gunnarsson, H. Handschuh, P. S. Bechthold, B. Kessler, G. Ganteför, and W. Eberhardt, Phys. Rev. Lett. **74**, 1875 (1995).

[30] G. Schulze Icking-Konert, H. Handschuh, P. S. Bechthold, G. Ganteför, B. Kessler, and W. Eberhardt, Surface Review and Letters 3, 483 (1996).

[31] M. Willis, M. Götz, A. K. Kandalam, G. F. Ganteför und P. Jena, Angew. Chem. Int. Ed. **49**, 8966 (2010).

[32] STEM group

[33] STEM group

Figure Captions

Fig. 1

PACIS source with the annealing stage and the setup for neutral cluster deposition on a TEM grid.

Fig. 2

Typical mass spectra of annealed $W_nS_m^-$ and $Mo_nS_m^-$ cluster anions generated with the PACIS equipped with the annealing stage. With the annealing switched off, just one broad maximum is observed (not shown).

Fig. 3

The position of the second maximum depends on the source parameters. It can easily be shifted to larger masses. At lower masses there seems to exist a minimum size corresponding to the mass of approximately 60 monomer units. If the parameters are optimized to shift the maximum to a size below ~ 80 monomers, it becomes weaker and disappears.

Fig. 4

Photoelectron spectra of cluster anions within the second maximum recorded with a photon energy of 7.9 eV. The mass resolution is not sufficient to resolve individual masses. Therefore, the mass range has been covered by a systematic scan. The mass is given in amu for each spectrum. The red line is an average. With increasing mass, the position of the broad maximum shifts to higher binding energy.

Fig. 5

High resolution bright field (a) and annular dark field (b,c) scanning transmission electron microscope images of W_nS_m particles deposited on a silicon oxide TEM grid. The deposited material is agglomerated in larger lumps of material. The images show only bulk-like layered structures. At maximum resolution (2nm scale bar) individual metal atoms can be discerned (white dots). Stacks of very small platelets can be identified (white ellipse).

Fig. 6

Picture of a scanning tunneling microscope operated in ultrahigh vacuum of $Mo_nS_m^-$ cluster anions deposited at high kinetic energies (3-7eV/atom). The clusters are pinned to defects on the terraces of the HOPG created by the impact. The height of the particles corresponds

roughly to the thickness of a single layer of MoS_2.

Fig. 7

STM picture of $Mo_nS_m^-$ clusters deposited on HOPG at lower kinetic energy (0-3eV/atom). The clusters diffuse to step edges. The height scans indicate a height corresponding to the thickness of a MoS_2 platelet.

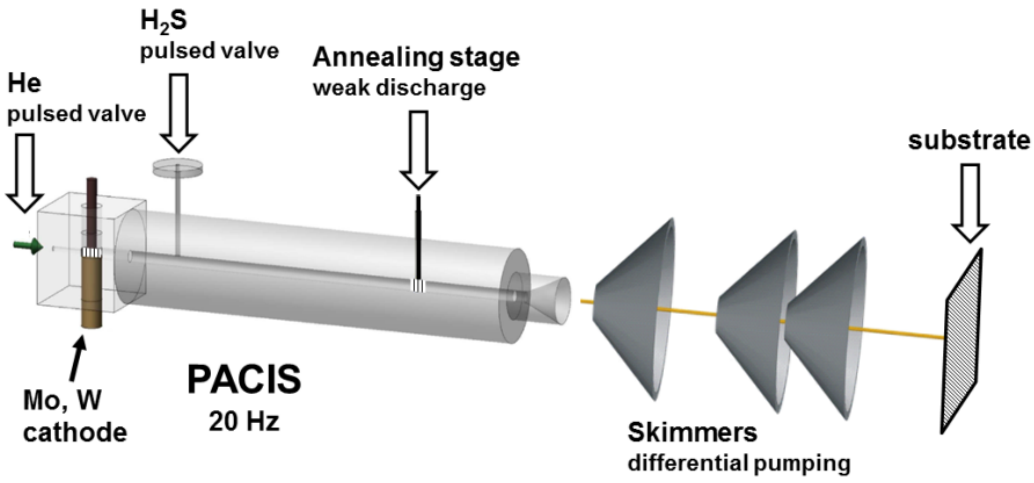

Fig. 1

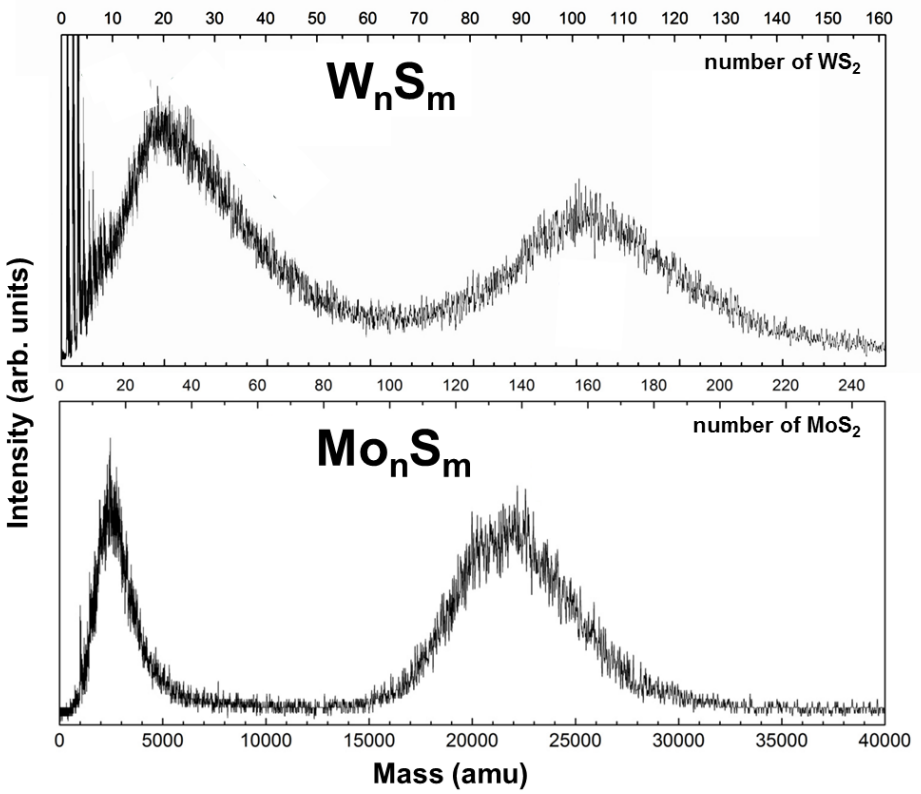
W_nS_m
number of WS2
Mo_nS_m
number of MoS2
Intensity (arb. units)
Mass (amu)
0 10 20 30 40 50 60 70 80 90 100 110 120 130 140 150 160
0 20 40 60 80 100 120 140 160 180 200 220 240
0 5000 10000 15000 20000 25000 30000 35000 40000

Fig. 2

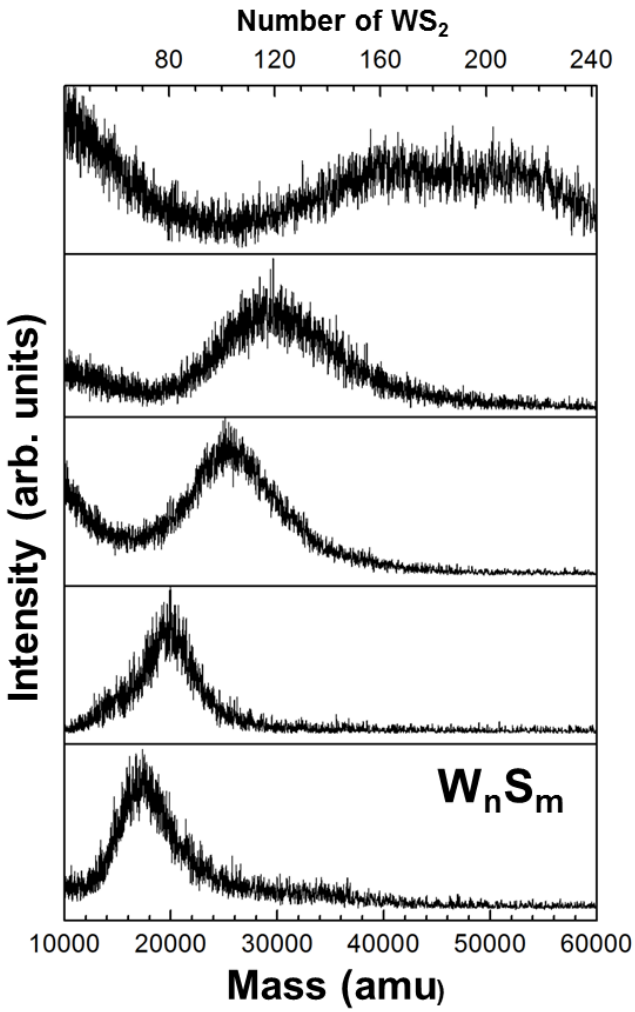
Number of WS2
80
120
160
200
240
Intensity (arb. units)
WnSm
10000
20000
30000
40000
50000
60000
Mass (amu)

Fig. 3

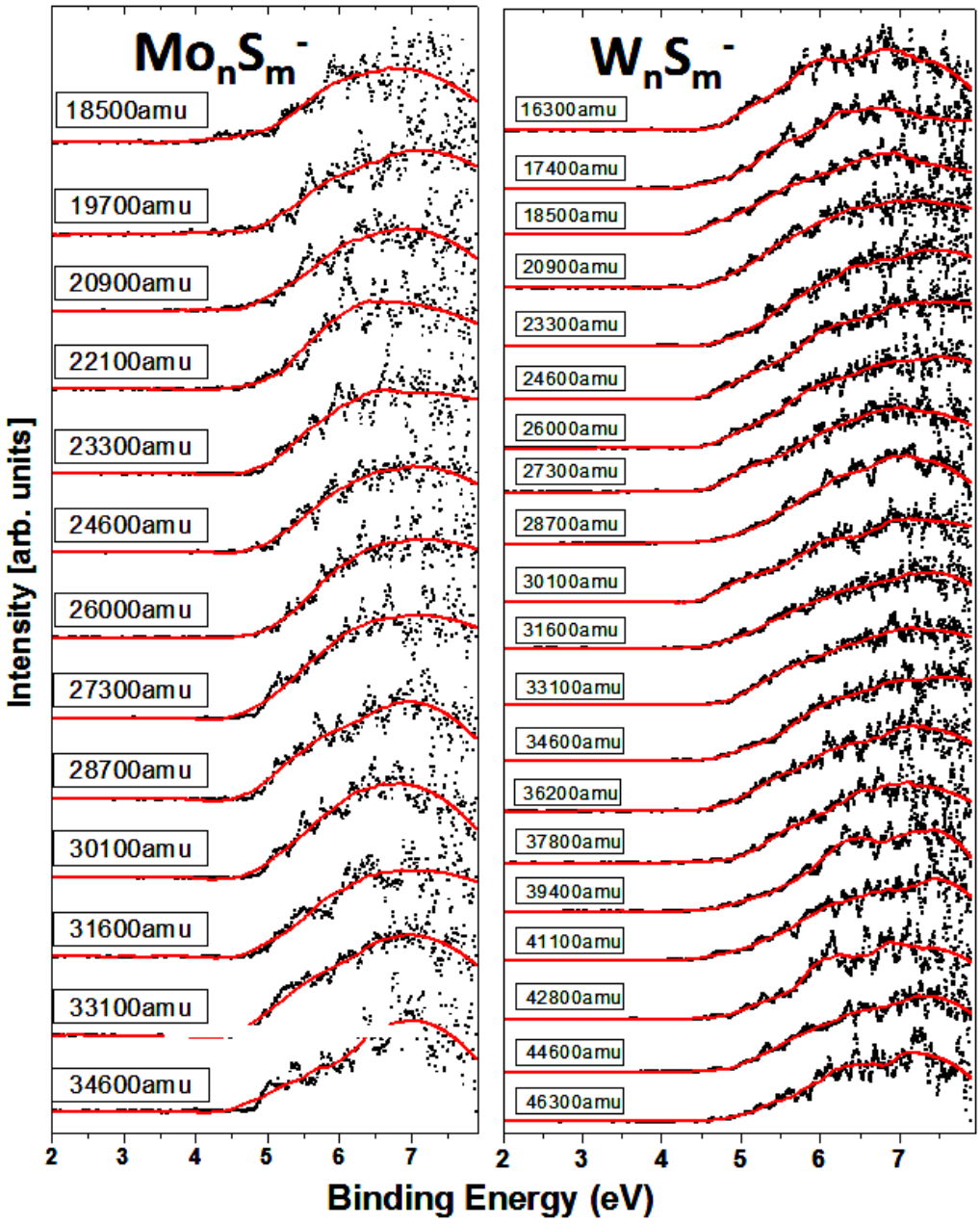
$Mo_nS_m^-$
18500amu
19700amu
20900amu
22100amu
23300amu
24600amu
26000amu
27300amu
28700amu
30100amu
31600amu
33100amu
34600amu
$W_nS_m^-$
16300amu
17400amu
18500amu
20900amu
23300amu
24600amu
26000amu
27300amu
28700amu
30100amu
31600amu
33100amu
34600amu
36200amu
37800amu
39400amu
41100amu
42800amu
44600amu
46300amu
Intensity [arb. units]
2
3
4
5
6
7
Binding Energy (eV)

Fig. 4

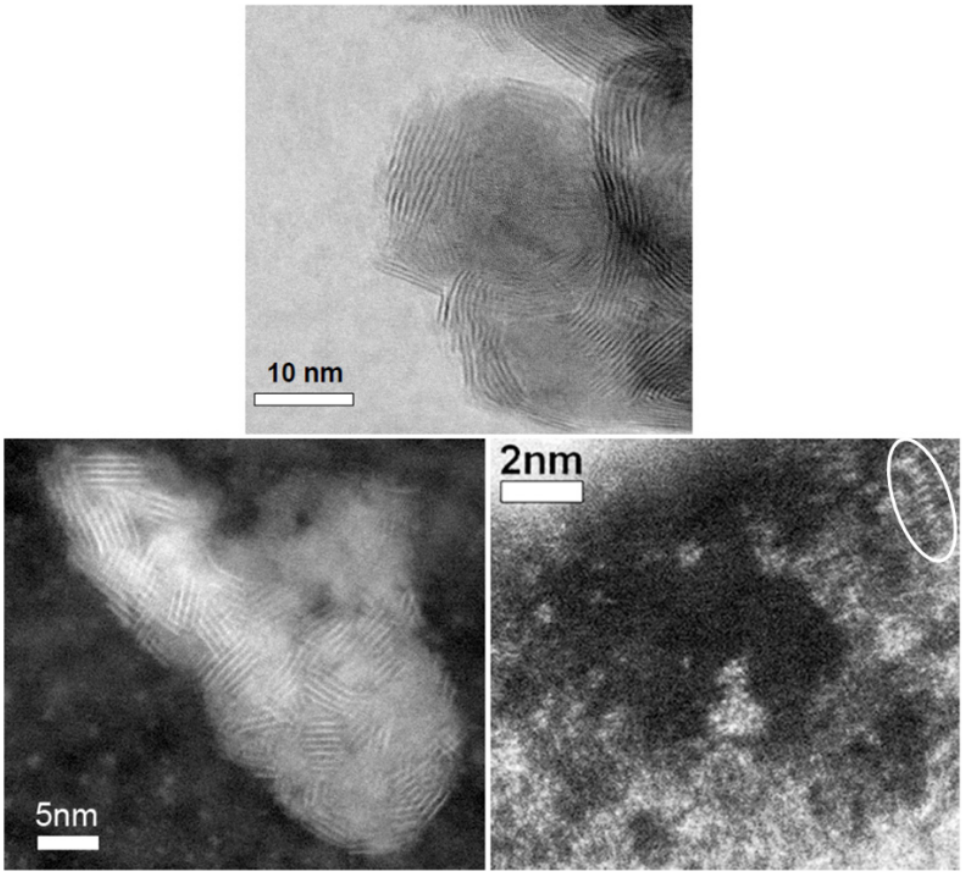

Fig. 5

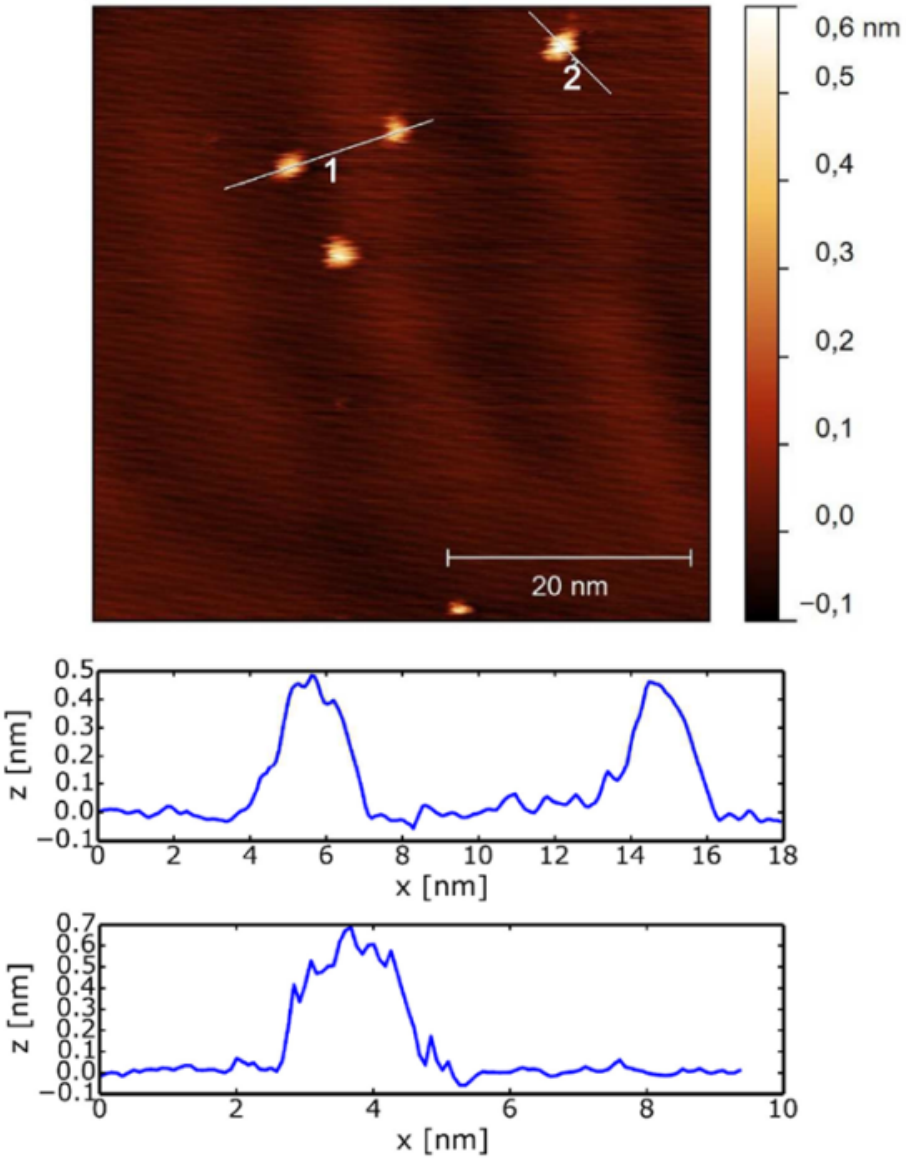

Fig. 6

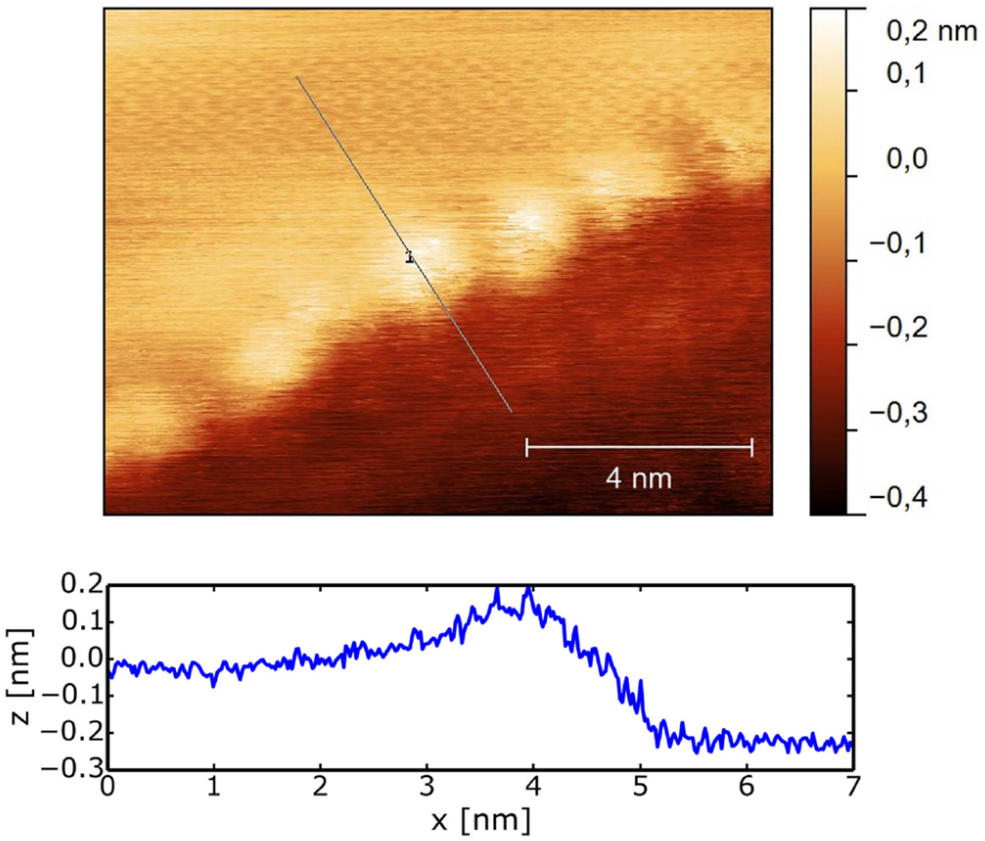

Fig. 7